BULLET: Jurnal Multidisiplin Ilmu
Volume 01, No. 02, April-Mei 2022
ISSN 2829-2049 (media online)
Hal 203-208

Analysis of Key Parameters and Mesh Optimization in Computational Fluid Dynamics Using Open FOAM

Syed Muhammad Asif

Queen Mary University of London

sm.asif@hotmail.com

Abstract

The aim of this report is to display and explain the results obtained using open source Computational Fluid Dynamics solver i.e. Open FOAM, when few key parameters were computed and an in-depth comparison is made between different mesh sizes and their quality. Few key parameters that were examined included total pressure, static pressure, lift coefficients and drag coefficients. This report also discusses the validity of the results that were obtained and goes on to deduce the mesh that is favorable for this particular simulation.

Keywords: Open FOAM, Computational Fluid Dynamics (CFD), mesh quality, mesh size, total pressure, static pressure, lift coefficient, drag coefficient, simulation validation, mesh optimization.

INTRODUCTION

Computational Fluid Dynamics (CFD) normally involves the analysis of fluid flow by means of computer based simulation. Most commercial CFD software's have three main elements [1].

1) Pre-processor
2) A solver
3) Post-processor

'Pre-processing allows the input of a flow problem to a CFD program. This is achieved through a user friendly interface. After the data has been input in to the system, the data undergoes transformation which makes it suitable to be used by the solver [2].

'Solver uses finite volume method for numerical calculations. The algorithms consist of the following steps [3].

1) Integration of all equations over all the finite control volumes of the domain.
2) Discretization – conversion of the resulting integral equations into a system of algebraic equations.
3) Solution of the algebraic equations by an iterative method [1].

Post-processing consists of data analysis through visualization. This may also include animations and charts. The software used for this particular application was Open FOAM. It uses Linux operating system for the commands to be manually fed in to it. Open FOAM used Helix as its graphical interface [4]. It significantly simplifies entering flow and solver parameters. Preview was used for data analysis and visualization. It is an open source application and allows users to build their own visualizations of their data using qualitative and quantitative technique [5].

PRE-PROCESSING

The flow and solver parameters were entered using Helix graphically. Fluid chosen is air. The flow is chosen to be steady, incompressible, in viscid and laminar. In viscid case is achieved by setting dynamic and kinematic viscosity as zero. For the case to run effectively, it is essential that the boundary conditions are properly imposed. Gauge pressure at outlet is selected zero [6]. Since this value is not represented by a single number, 'zero-gradient' is more appropriate here. At inlet, the conditions are reversed to that of the outlet. At the inlet, velocity vector is imposed. Given our angle of attack, the y-component is $\sin(\alpha)\, v_\infty = 3.0878 ms^{-1}$, the x-component is $\cos(\alpha)\, v_\infty = 58.919 ms^{-1}$ and the z-component is zero. As previously stated, gauge pressure at inlet is not imposed [7].

Since the 'fixed wall' condition is selected for wing profile, it is important that the 'slip' wall type is selected. This is because the 'fixed wall' condition for in viscid flow imposes that the flow is tangent, but it can slide past the wall without viscosity. The solver setting is set as 'simple'. In 'Runtime Controls' the number of iterations are specified. It is 0 for the Start time and 300 for the End time. More settings were slightly modified which included the lift and drag values [8].

BULLET: Jurnal Multidisiplin Ilmu
Volume 01, No. 02, April-Mei 2022
ISSN 2829-2049 (media online)
Hal 203-208

RESULTS

Effect of mesh refinement and 2nd order accuracy

	1st order	2nd order
128	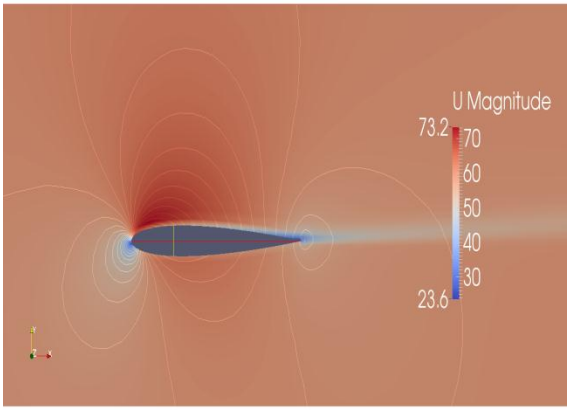	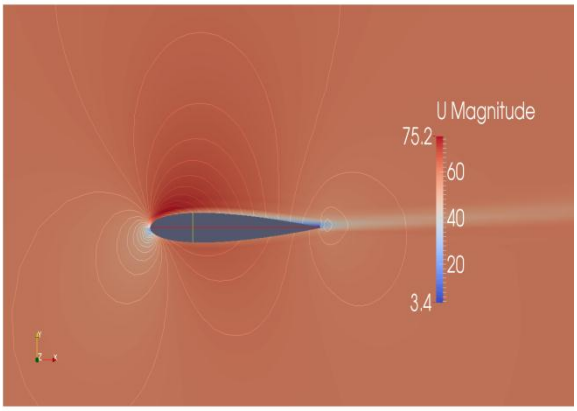
256	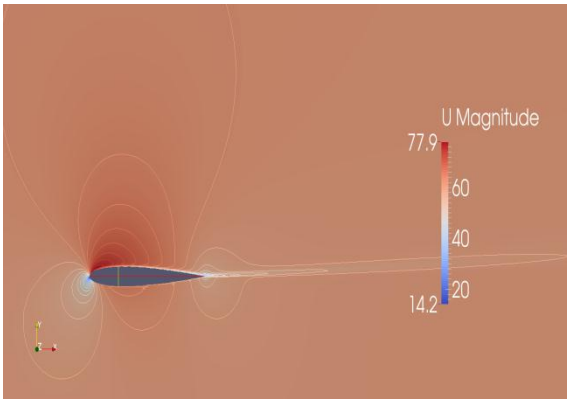	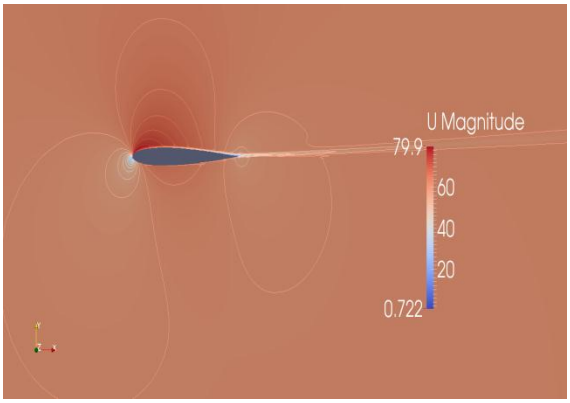
512	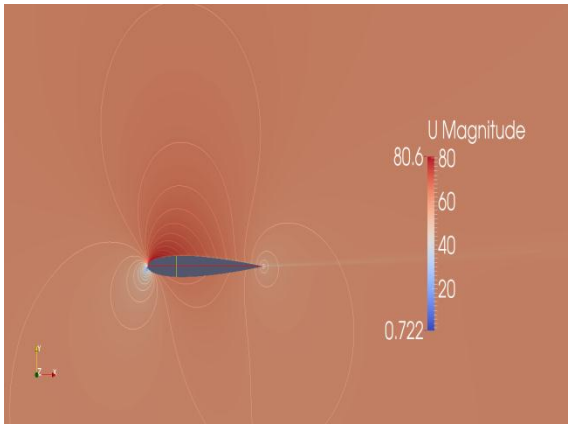	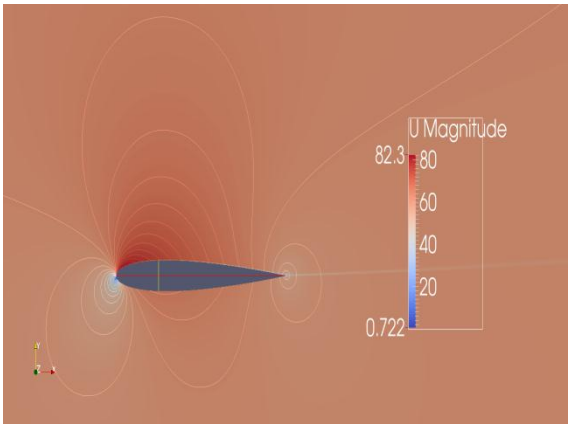

The number of meshes determines the accuracy of the results. Increasing the number of meshes will increase the accuracy of the results produced. Decreasing the number of meshes will decrease the accuracy of the meshes produced. Increasing the number of meshes require significant increase in the demand of processing power. Thus more powerful computers are needed which increases the cost. Moreover, it also increases the amount of time it takes to process [9]. Thus it is very important to balance between accuracy and number of meshes. To illustrate the difference between accuracy and the number of meshes, few diagrams are added.

If the diagrams above are observed carefully, it can be noticed that the velocity contours become more round in shape. This is more noticeable at the tail. As the order of the case is increased, the resolution of the stagnation point is also increased. This is primarily because there are greater mesh sizes having more cells concentrated at the leading edge [10].

BULLET: Jurnal Multidisiplin Ilmu
Volume 01, No. 02, April-Mei 2022
ISSN 2829-2049 (media online)
Hal 203-208

Moreover, it can see that the flow characteristics change in different figures shown above. The changes occur primarily because of artificial viscosity. Velocity drop has occurred due to artificial viscosity. As the order of accuracy is increased, artificial viscosity drops [11]. This is clearly illustrated by the pictures above. As the order of accuracy increases due to mesh refinement, the boundary layer thickness becomes smaller which is thus responsible for decreasing the error that occurred to due reduction in artificial viscosity. As a conclusion, lesser the artificial viscosity is used, more accurate results are produced [12].

Graph 1.1 below illustrates that when second order cases are compared to their first order cases, there exist more energy loss in second order. This is incorrect because second order cases should have reduced pressure loss due to reduced truncation error. This is primarily due to software fault.

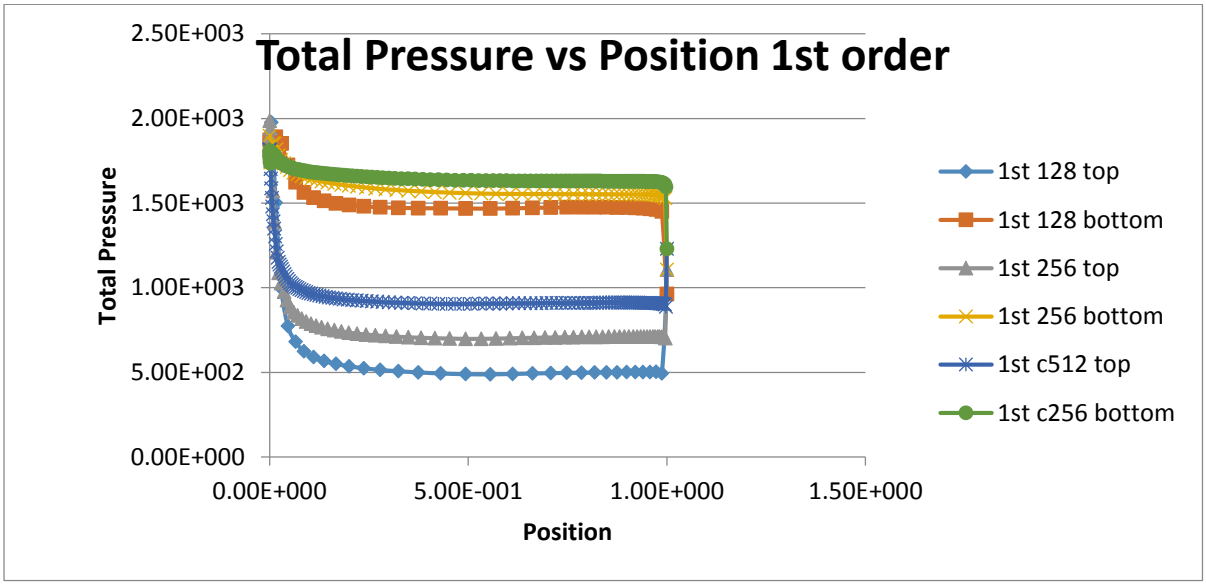

Diagram 1.1Total pressure vs position 1st order

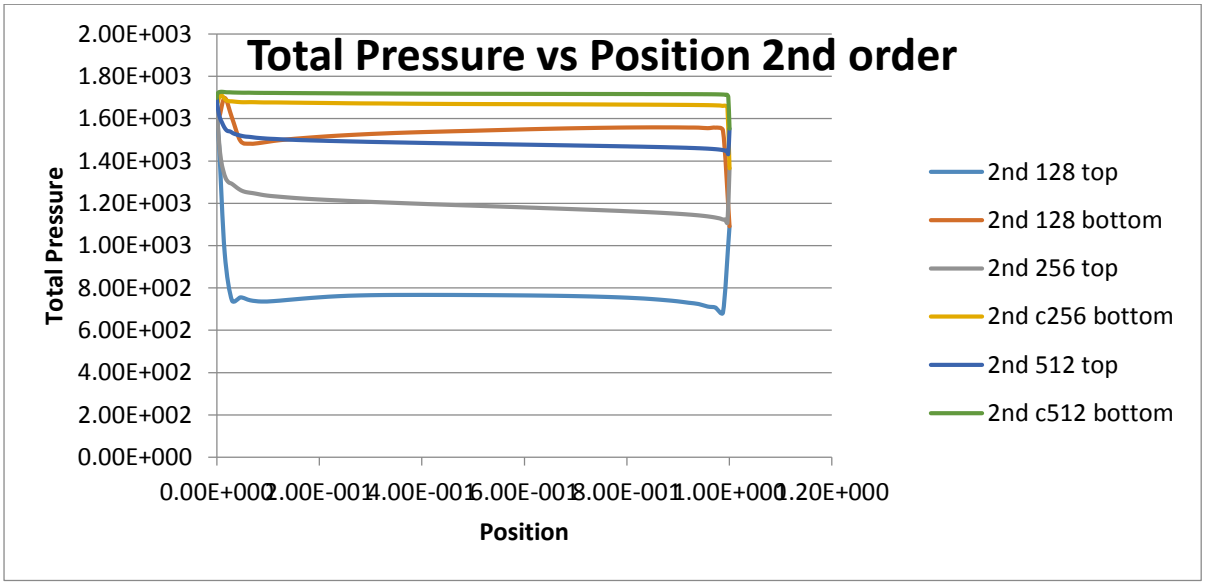

Diagram 1.2 Total pressure vs position 2nd order

BULLET: Jurnal Multidisiplin Ilmu
Volume 01, No. 02, April-Mei 2022
ISSN 2829-2049 (media online)
Hal 203-208

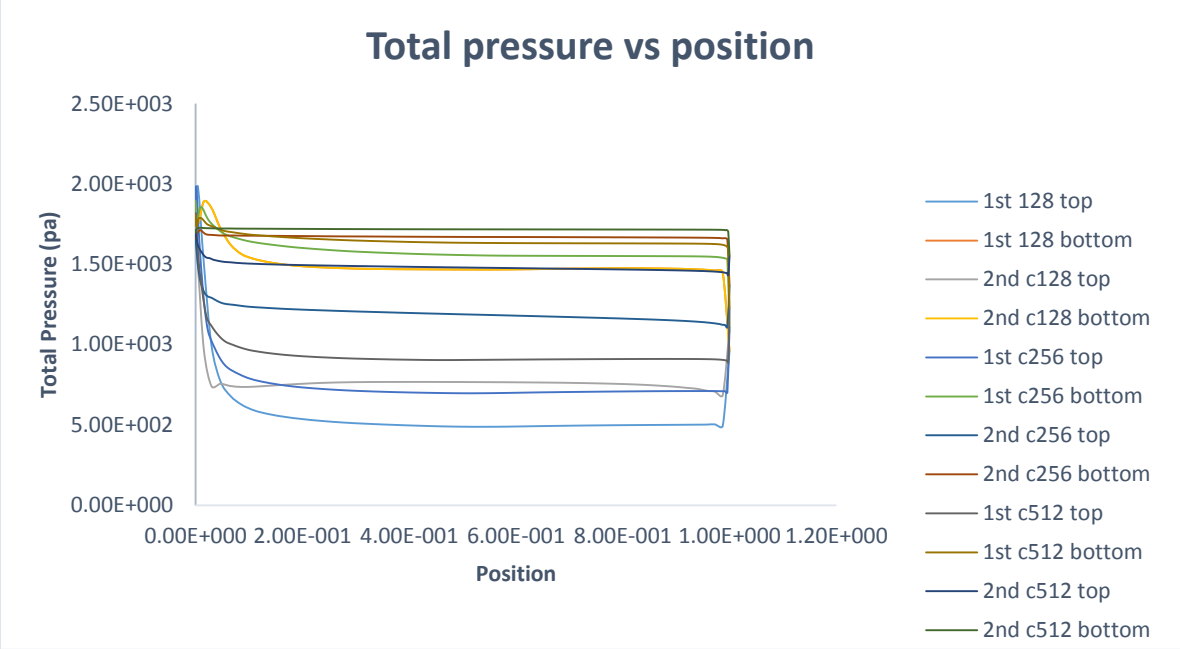

Diagram 1.3 Total pressure vs position

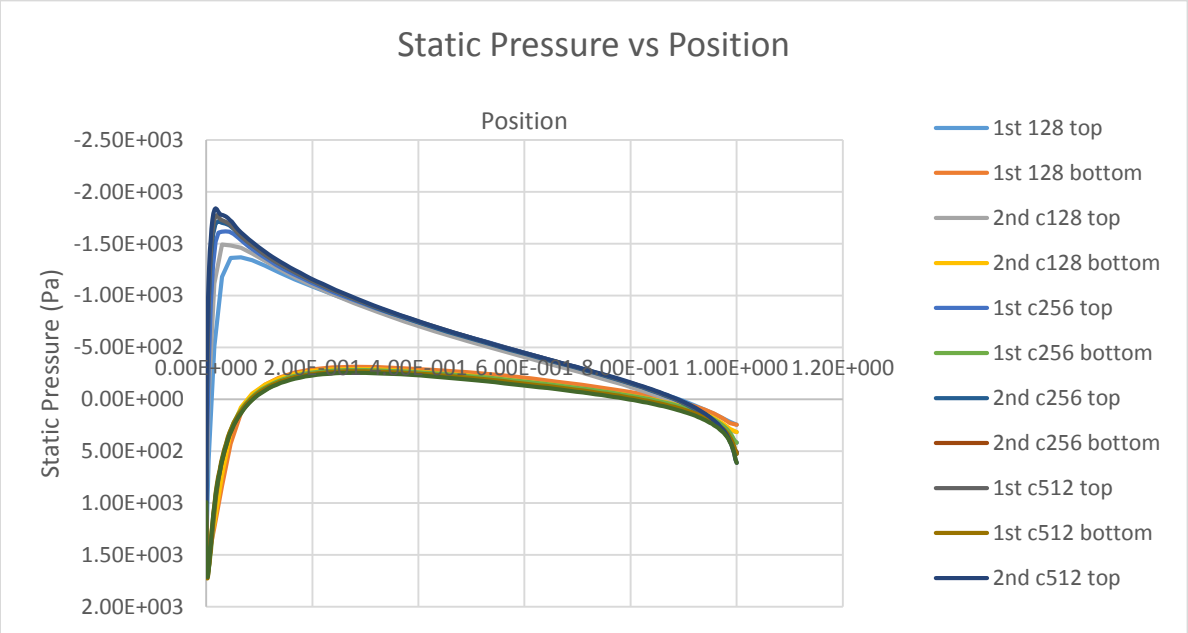

Diagram 1.4 Static Pressure vs Position

Mesh size	Order	Cl	Cd
128	1	0.318	0.0229
128	2	0.281	0.0136
256	1	0.356	0.0143
256	2	0.312	0.00213

Chart 1.1

DISCUSSION

Provided cases: There seem to be obvious differences between different levels of mesh refinements. C128 cases have much thicker boundary layer. Theory predicts that there should be no boundary layer. But this boundary layer is created due to artificial viscosity. Artificial viscosity also effects drag [13]. Chart 1.1 above displays this phenomenon. As the mesh refinement is increased, drag decreases. Since the flow is inviscid and 'no-slip' option is selected, there should be no drag at all. This drag exist primarily due to high level of artificial viscosity that is present in our simulation [14].

Comparison of own against provided simulation: When the results of my C256 2nd order mesh is compared with the provided case, there exist few differences among them. The stagnation point seem to be more protruding of my own case [15]. It is also evident that my case has less artificial viscosity because of smaller boundary layer. Contour lines are less circular and expanded. Higher loss of pressure is also seen in the static pressure graph [16]. This concluded that the velocity for my particular case might be higher than the one in provided case. This also has a connection with artificial viscosity. Artificial viscosity should thus be higher in the provided case which caused a greater drop in the velocity [17].

Comparison of Total Pressure and Lift and Drag values

Size	Case	Order	Cl	Cd
256	My Case	2	0.3319	0.00248
256	Provided Case	2	0.2943	0.00478

Chart 1.2 Drag and Lift coefficients: Chart 1.2 above shows drag and lift coefficients of my own case and the provided case. Although the values fall in a certain range, but the drag coefficient of my case is higher than the provided case whereas the lift coefficient of my case is greater than the lift coefficient of the provided case. The results of my case seems to be better since less drag and high lift is ultimately what we want [18]. As for the provided case, it is once again evident that there must be greater artificial viscosity in it. This is because viscosity cause the drag to increase and since the flow in inviscid, there should not be any drag, and thus comes the concept of artificial viscosity [19]. Total pressure is effectively a measure of energy. Therefore, when 2nd order total pressure is analysed for my own simulation, it is observed that again the pressure loss for second order is greater than the first order. This should not be the case. Although, artificial viscosity could be one reason as to why it has happened [20].

CONCLUSION

Critical analysis of the results suggest that the most accurate solution is 2nd order C512 mesh solution. Besides the fact that this mesh has a high error in Total Pressure, it displays excellent accuracy of the static pressure and lift and drag values. Moreover, the increased mesh size does help to reduce the error in Total Pressure.

I believe that I have come up with an accurate solution but clearly the time given was, in my opinion, not enough to produce a trustworthy result. But by gaining more experience in the future, I am confident to produce more sound results.

REFERENCES

1. An introduction to Computational Fluid Dynamics, The Finite Volume Method, Second edition, by H K Versteeg & W Malalasekera.
2. Queen Mary University of London, DEN331 Computer Aided Engineering in Fluids and Solids, Computational lab assignment on CFD hand-out.
3. Hoppe, H., DeRose, T., Duchamp, T., McDonald, J., & Stuetzle, W. (1993, September). Mesh optimization. In *Proceedings of the 20th annual conference on Computer graphics and interactive techniques* (pp. 19-26).
4. Cignoni, P., Montani, C., & Scopigno, R. (1998). A comparison of mesh simplification algorithms. *Computers & Graphics*, *22*(1), 37-54.
5. Wang, Y., Pang, Q., Li, M., & Liu, Y. (2024). Comparative Study of Algorithms for the Conversion From Surface Mesh Models to Volume Mesh Models. *Advances in Civil Engineering*, *2024*(1), 4669855.
6. Allaire, G., Dapogny, C., & Frey, P. (2014). Shape optimization with a level set based mesh evolution method. *Computer Methods in Applied Mechanics and Engineering*, *282*, 22-53.
7. Secco, N. R., Kenway, G. K., He, P., Mader, C., & Martins, J. R. (2021). Efficient mesh generation and deformation for aerodynamic shape optimization. *AIAA Journal*, *59*(4), 1151-1168.

8. Wang, C., Zhao, Z., Zhou, M., Sigmund, O., & Zhang, X. S. (2021). A comprehensive review of educational articles on structural and multidisciplinary optimization. *Structural and Multidisciplinary Optimization*, 1-54.
9. Keshavarzzadeh, V., Alirezaei, M., Tasdizen, T., & Kirby, R. M. (2021). Image-based multiresolution topology optimization using deep disjunctive normal shape model. *Computer-Aided Design*, *130*, 102947.
10. Sushma, M. B., Roy, S., & Maji, A. (2022). Exploring and exploiting ant colony optimization algorithm for vertical highway alignment development. *Computer-Aided Civil and Infrastructure Engineering*, *37*(12), 1582-1601.
11. Lin, B., Chen, H., Yu, Q., Zhou, X., Lv, S., He, Q., & Li, Z. (2021). MOOSAS–A systematic solution for multiple objective building performance optimization in the early design stage. *Building and Environment*, *200*, 107929.
12. Sanil, G., Prakash, K., Prabhu, S., Nayak, V. C., & Sengupta, S. (2023). 2d-3d facial image analysis for identification of facial features using machine learning algorithms with hyper-parameter optimization for forensics applications. *IEEE Access*, *11*, 82521-82538.
13. Martins, J. R. (2022). Aerodynamic design optimization: Challenges and perspectives. *Computers & Fluids*, *239*, 105391.
14. Mei, B., Barnoon, P., Toghraie, D., Su, C. H., Nguyen, H. C., & Khan, A. (2022). Energy, exergy, environmental and economic analyzes (4E) and multi-objective optimization of a PEM fuel cell equipped with coolant channels. *Renewable and Sustainable Energy Reviews*, *157*, 112021.
15. Ma, X., Su, J., Wang, C., Zhu, W., & Wang, Y. (2023). 3d human mesh estimation from virtual markers. In *Proceedings of the IEEE/CVF Conference on Computer Vision and Pattern Recognition* (pp. 534-543).
16. Vidakis, N., David, C., Petousis, M., Sagris, D., & Mountakis, N. (2023). Optimization of key quality indicators in material extrusion 3D printing of acrylonitrile butadiene styrene: The impact of critical process control parameters on the surface roughness, dimensional accuracy, and porosity. *Materials Today Communications*, *34*, 105171.
17. Marinić-Kragić, I., Vučina, D., & Milas, Z. (2022). Global optimization of Savonius-type vertical axis wind turbine with multiple circular-arc blades using validated 3D CFD model. *Energy*, *241*, 122841.
18. Guan, S., Xu, J., He, M. Z., Wang, Y., Ni, B., & Yang, X. (2022). Out-of-domain human mesh reconstruction via dynamic bilevel online adaptation. *IEEE Transactions on Pattern Analysis and Machine Intelligence*, *45*(4), 5070-5086.
19. Nayak, J., Swapnarekha, H., Naik, B., Dhiman, G., & Vimal, S. (2023). 25 years of particle swarm optimization: Flourishing voyage of two decades. *Archives of Computational Methods in Engineering*, *30*(3), 1663-1725.
20. Ghorbani, E., Moosavi, M., Hossaini, M. F., Assary, M., & Golabchi, Y. (2021). Determination of initial stress state and rock mass deformation modulus at Lavarak HEPP by back analysis using ant colony optimization and multivariable regression analysis. *Bulletin of Engineering Geology and the Environment*, *80*, 429-442.